Scanning Microscopy

Volume 1994
Number 8 *The Science of Biological Microanalysis*

Article 29

1-27-1994

Optical Methods for Imaging Ionic Activities

Roger B. Moreton
Cambridge

Scanning Microscopy Supplement 8, 1994 (pages 371-390) 0892-953X/94$5.00+.25
Scanning Microscopy International, Chicago (AMF O'Hare), IL 60666 USA

OPTICAL METHODS FOR IMAGING IONIC ACTIVITIES

Roger B. Moreton

The Babraham Institute, Laboratory of Molecular Signalling, Department of Zoology
Downing Street, Cambridge CB2 3EJ, UK.
Telephone number.: (0) 223 336675.

(Received for publication November 3, 1993, and in revised form January 27, 1994)

Abstract

Optical fluorescence is characteristic of molecules and their environment, and dyes can be made whose fluorescence is altered by reversible binding to specific ions. By introducing these into the cytosol, fluorescence microscopy can be used to form dynamic images of ionic activities in living cells under experimental manipulation. Optical fluorescence spectra are broad-band, and if specific ion binding alters the wavelength of maximal excitation or emission, quantitative measurements can be made from the ratio of images taken at two different wavelengths, eliminating errors due to spatial variations in dye concentration and optical path-length. This method is analogous to continuum normalisation in X-ray microanalysis, and is implemented using a sensitive video camera and computer processing of digitised images. Fluorescent indicators exist for calcium, magnesium, hydrogen, sodium, zinc and chloride ions. Most imaging work has been on calcium, which is important in many cell signalling processes, and several calcium indicators are available with different spectral properties. Spatial resolution is limited to a few μm by out-of-focus blur, but repeated images can be captured with a time resolution as low as 200 msec, and by using dyes with high binding affinity, detection limits can be lower than by X-ray methods. There is a large and fast-growing literature of applications to many plant and animal cell-types.

Key Words: Optical fluorescence, optical microscopy, digital imaging, CCD camera, intracellular ions, quantitation, calcium, pH, cell biology, cell signalling.

Introduction

The subject of this paper is the use of fluorescent dyes to measure ionic activities inside cells. By analogy with electron-probe techniques, it could reasonably be called photon-probe microanalysis, and in a later section I shall briefly compare the capabilities of optical and electron-probe measurements, which are in many ways complementary. An important difference is that the electron-probe interacts directly with atoms intrinsically present in the cell, whereas optical probes generally (though not always) require the introduction of a specialised, extrinsic dye into the cell. Thus in fluorescence measurements there are really two probes: the dye, and the photons used to excite it. This is a drawback in that the scope of the method is limited by the availability of indicator-dyes; but against this is the enormous advantage that optical probes can be used in solutions exposed to the normal room atmosphere so that ion activities can be monitored in living cells during the course of experimental manipulation. This capability for providing specific and dynamic information about the contents of living cells has lead to a great revival of interest in optical microscopy in the last decade or so.

The use of optical probes to measure ionic activities inside cells is not in itself new. Shimomura *et al.* (1962) described a protein Aequorin which can be extracted from some hydromedusan jelly-fish, and whose chemiluminescence has been used to measure intracellular calcium since about 1970 (Ashley and Ridgway, 1970; Campbell and Sala-Newby, 1993); and the metallochromic dyes known as Arsenazo-III (Dipolo *et al.*, 1976; Brown *et al.*, 1977) and Antipyrylazo-III (Kovacs *et al.*, 1979) have been used since the mid 1970s to measure calcium from changes in their absorption spectrum. However, the luminescence of Aequorin is too faint, and the percentage changes in absorbance of the Arsenazo-type dyes are too small, to provide useful signals from anything other than quite a large volume of cell-contents, and their use has generally been restricted to monitoring average ion activities over large cells such as squid giant axons (Dipolo *et al.*, 1976), molluscan neurons (Gorman and Thomas, 1978), and giant muscle-fibers from the barnacle *Balanus nubilis* (Ashley and

Ridgway, 1970), or in fiber-bundles from vertebrate muscle (Kovacs *et al.*, 1979). The signals are too weak to provide detailed images in any reasonable acquisition-time.

The real break-through came with the development of fluorescent indicators of which the first was the calcium-chelating tetracarboxylate known as Quin-2, reported by Tsien *et al.* (1982). Fluorescent indicators have the advantage over absorption indicators, that with suitable experimental design the fluorescence can be measured against a dark background, as opposed to absorbance which is recorded as a small change - never more than 1 or 2 per cent - in a large background of transmitted light. Thus it is relatively easy to obtain a strong enough signal to form useful images. Despite this, the intensity of fluorescence is seldom bright enough to be more than barely perceptible to the dark-adapted human eye, and the advance of imaging techniques has depended on the development of sensitive video cameras, as well as the improvement and expanding range of available dyes.

In biology the bulk of the literature on imaging of intracellular ions has been concerned with calcium: the literature is far to extensive to be summarised here, but the three general books cited below give some representative references, and an entire issue of the journal Cell Calcium (Volume 11, Parts 2/3 Feb/Mar 1990) was devoted to the technique and practice of intracellular calcium imaging. The reasons for this are firstly, that calcium turns out to be universally important in cell signalling, from nerve and muscle signals, through hormonal messages, down to the contact and positional information conveyed between cells during development of an organism; and secondly that intracellular calcium activities (as opposed to concentrations) are generally too low - in the range of tens of nanomolar - to be easily measured by other means such as ion-selective electrodes. However the range of intracellular indicator-dyes is constantly expanding, and probes are now available for pH, sodium, magnesium and chloride, as well as for some non-ionic components of the cell signalling pathway such as cyclic AMP (Adams *et al.*, 1991, 1993) and protein kinase-C (Poenie and Chen, 1993). It is also possible to attach fluorescent moeities to cell constituents such as the specialised calcium-binding protein Calmodulin (Hahn *et al.*, 1990), to the endoplasmic reticulum (Terasaki, 1993), or to the myosin components of the cytoskeleton (Sawin *et al.*, 1993), so that their position and physico-chemical state can be monitored during development and functioning of the cell; and the dependence of optical fluorescence upon the physical environment of the fluorescent molecule can be used to monitor parameters such as viscosity of the cellular medium (Luby-Pheols *et al.*, 1993), or structure and rigidity of lipid domains in a cell membrane (Florine-Casteel *et al.*, 1993; Kok and Hoekstra, 1993).

I shall begin by outlining the principles underlying design and use of optical fluorescence to monitor ion activities. I shall then describe the basic techniques for using fluorescent probes to monitor or image ionic activities in cells, with a summary of quantitation methods, and some illustrative results in cell biology. There follows a consideration of the limitations and sources of error in the method. Finally the technique will be compared with electron-probe microanalysis, with the aim of showing how the two methods are complementary to one another. Much of the technical material on fluorescence microscopy and quantitative imaging has been collated and discussed in three excellent books published this year, and edited respectively by Herman and Lemasters (1993), Mason (1993) and Shotton (1993): reference is made to individual chapters in these, as appropriate. See also Tsien and Harootunian (1990); Moreton (1991; 1992) for a more detailed discussion of some of the issues raised in this paper.

Monitoring Ion Activity with Fluorescent Probes

Optical fluorescence occurs when a molecule absorbs a photon by transferring its energy to an electron, which then decays to the ground state after a few nano-seconds by emitting a second photon of lower energy. Absorbed photons are most often in the blue or ultra-violet region, with wavelengths in the band between 300 and 500 nm. The difference between absorption and emission energies is known as the Stokes shift, and is accounted for by intermediate transitions among different vibrational states of the molecule. It allows the exciting and emitted photons to be separated, so that the fluorescence intensity can easily be measured. Kasten (1993) gives a brief account of the nature of optical fluorescence, and the history and development of fluorescent dyes.

Because the excitation light is of relatively low energy - about 3 eV per photon at a wavelength of 400 nm, for example - optical fluorescence typically involves only the outermost atomic electrons, in complex molecules with many possible vibrational states. Thus in contrast to electron-induced X-ray emission, optical fluorescence can generally be excited by photons over a broad wavelength-band, and the spectrum of emitted photons is similarly broad; and whereas X-ray emissions are characteristic of atoms and largely independent of their environment, optical fluorescence is a property of molecules and is strongly sensitive to their physical and chemical environment. Thus it is possible to design

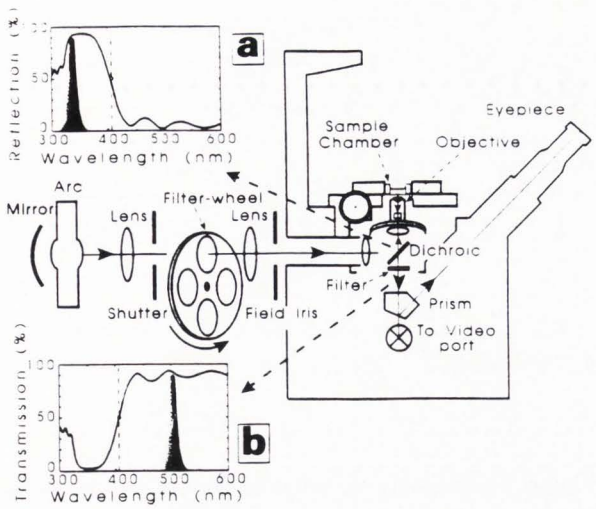

Figure 1: Dual-wavelength epi-fluorescence imaging. Light from a single arc-lamp passes through a rotating filter-wheel so that excitation wavelengths can be alternated by using different band-pass optical filters. Insert (a) - shorter wavelengths are reflected by the dichroic mirror, so that the waveband selected by the excitation filter (shown shaded) is passed through the objective, which condenses it into the specimen. Insert (b) - longer wavelength fluorescence from the specimen is transmitted by the dichroic mirror, and the appropriate waveband (shaded) is selected by the emission filter.

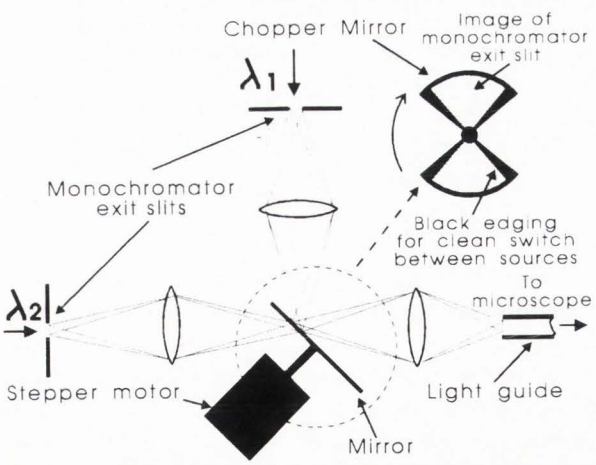

Figure 2: Using a rotating chopper-mirror to combine excitation from two monochromators. Real images of the two exit slits are focussed onto coincident positions on the mirror, so that light is alternately transmitted from one monochromator, or reflected from the other.

probe molecules with specific affinity for particular ions, association with which causes a change in electron-distribution, with consequent shifts in excitation or emission spectra. I shall examine probe design in a little more detail later on. At this stage it should be noted that, because ionic association is a reversible binding, it is the thermodynamic activity of the ion that is reported by the probe, not the concentration of its parent atom or molecule. This is another important difference from X-ray microanalysis, and obviously leads to the possibility of making complementary use of the two techniques.

Basic Technique: Digital Imaging by Epi-fluorescence Microscopy

In order to obtain an image of ion distribution, as reported by a fluorescent probe, all that is needed is to illuminate the sample at a suitable wavelength, and to collect and focus the emitted light into an image. For quantitative measurement on the image, it is then necessary to scan and digitise it, and this can be done in two ways. Either the excitation beam can be scanned, in a manner analogous to the scanning electron microscope, or the sample can be uniformly illuminated, collecting the image all together and scanning it by means of a video camera. Scanning the excitation beam is conveniently done by using a laser as a source, and leads to the technique of confocal laser scanning microscopy, which is the subject of another paper in this volume. The present paper will concentrate on the other, older method, which is called epi-fluorescence microscopy.

The technique of epi-fluorescence is well-established, and has been described in detail in a number of text books (Taylor *et al.*, 1986; Ploem and Tanke, 1987; Rost, 1991; Ploem, 1993). I shall give only a brief description here.

The epi-fluorescence microscope (Figure 1) is a standard optical microscope; the inverted configuration is convenient for experiments on live tissue. The heart of the system is a dichroic mirror which carries multiple layers of refracting material, such that destructive interference causes reflection of light below a certain wavelength, but transmission of longer wavelength light. Thus the objective lens can be used to condense light from an excitation source into a small region of the sample, and simultaneously to form an image from fluorescence arising in the same region. This efficient arrangement avoids unnecessary exposure and bleaching, and there is no need to re-focus the excitation light every time the microscope is focussed up and down; but for working with UV excitation it requires special objectives made of quartz or, less expensively, lithium glass. Inset is a transmittance spectrum for a typical dichroic mirror, designed for a "turn-over" wavelength of 400 nm. Short wavelength excitation light is reflected into the objective, but longer wavelength fluorescence is transmitted to the

eyepiece: a Stokes shift of at least 40 nm is needed to allow efficient separation.

The block carrying the dichroic mirror also carries an emission filter, designed to cut out unwanted light including stray reflected excitation light, and autofluorescence from endogenous cell constituents. This filter will again be of the interference type, either long-pass or band-pass, depending on the emission spectra of the fluorescent probes in use.

The light for exciting fluorescence will usually come from an arc lamp or a laser. Wavelengths needed for many of the indicators used in quantitative work are in the UV range - between 340 and 400 nm - so that for epi-fluorescence imaging either a mercury or a high-pressure xenon arc is generally used. The xenon arc gives a smoother spectrum over a useful range of wavelengths, but the mercury arc has several strong lines, including one at 366 nm which can be useful for exciting several indicator dyes. Lasers are less useful than arc lamps because of the limited range of wavelengths available at suitable intensities, particularly in the UV: the use of laser sources in fluorescence microscopy is largely restricted to confocal scanning work, where the special characteristics of laser light become much more important.

The excitation wavelength is selected either by a multi-layer interference filter, usually designed to transmit wavelengths over a 10 nm band, or by a monochromator using a diffraction grating.

Interference filters can be mounted on a wheel (Figure 1), allowing wavelengths to be changed rapidly during an experiment. It will become apparent that repeated alternation of excitation wavelengths is important in quantitative fluorescence imaging, so this is a useful feature. Also, if the cells are loaded with a mixture of dyes, two or more ions can be imaged simultaneously by using several different wavelengths in sequence (Bright, 1993a; Morris, 1993).

If monochromators are used then a rotating mirror is needed to switch between two light paths (Figure 2), and the choice of wavelengths for rapid switching is restricted to two. On the other hand grating monochromators can be tuned in the same way as grating X-ray spectrometers, so there is complete freedom to choose both centre wavelength and bandwidth, to suit any particular experiment, and the intensities of the two sources can be independently adjusted by altering slit-widths. With a filter-wheel, neutral-density filters are needed to make this adjustment.

Experiments on living cells are normally done in an aqueous medium, and although this can be done in an upright microscope using water-immersion objectives, an inverted microscope allows much easier access to the

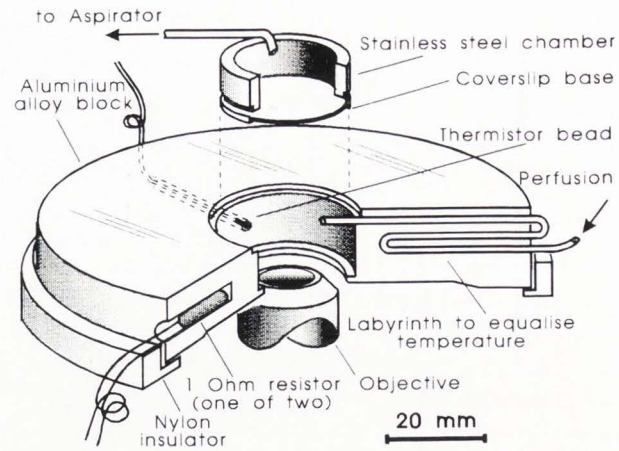

Figure 3: A simple temperature-controlled microscope stage.

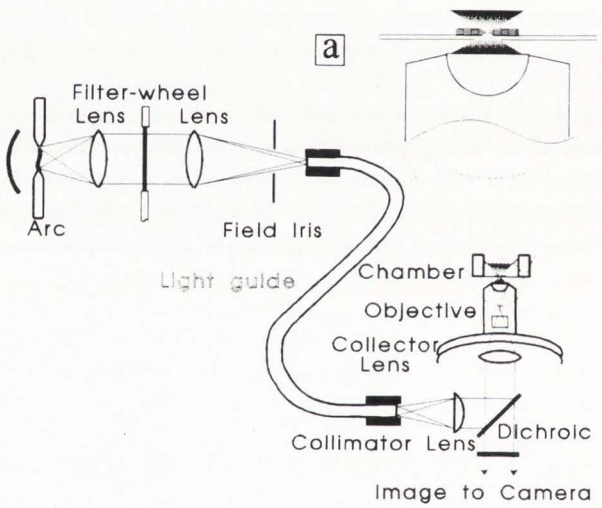

Figure 4: Epi-fluorescence illumination, with mechanical isolation of the microscope from the excitation-source. Light from an arc lamp is conducted to the microscope through a liquid light-guide or randomised quartz fibre-optic bundle. As well as providing mechanical isolation, this has the effect of "scrambling" the image of the arc or monochromator exit-slit, so that the field of view is uniformly illuminated. Insert (a) - the exciting radiation is concentrated by the objective, and illuminates a double-cone shaped region with the apex in the plane of focus. Emitted radiation is collected from a similar region.

cells for applying drugs, or for micropipette work involving micro-injection or electrophysiology (e.g., Niggli *et al.*, 1993). It is convenient to use cells attached to, or indeed cultured on, an ordinary microscope cover-

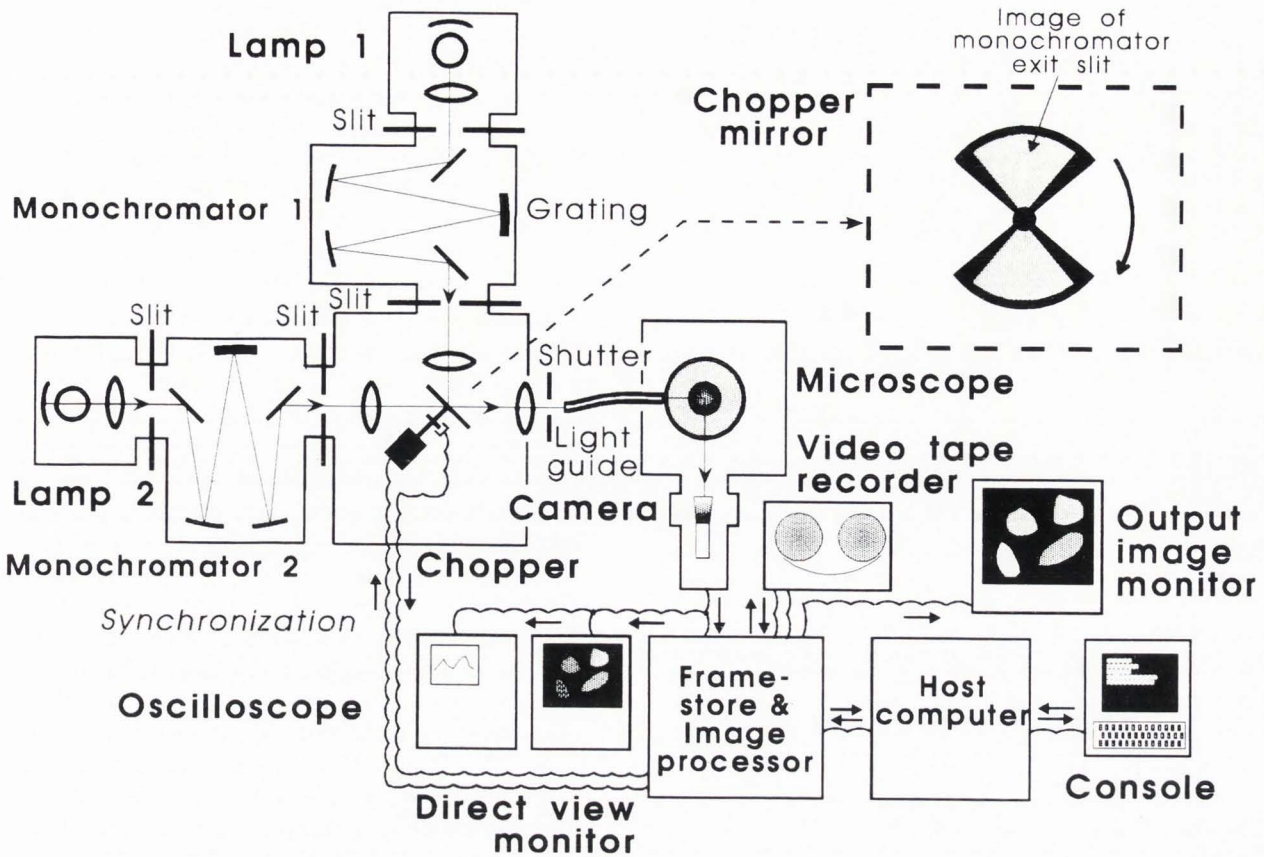

Figure 5: Summary-diagram of a complete system for dual-wavelength epi-fluorescence imaging. Excitation is derived from two independent arc lamps, with complete control over wavelength and bandwidth through twin grating monochromators. Light from these is selected alternately by a rotating chopper-mirror, and fed to the microscope through a flexible light-guide to provide mechanical isolation. Images collected alternately by a sensitive video camera are digitised by a frame-store and combined under computer control, to form a ratio-image directly representing ion-distribution in the cells.

slip, which can become the base of a perfusion chamber.

In the example shown in Figure 3 the microscope stage is replaced by a duralumin block whose temperature can be controlled by a simple feedback circuit, using a pair of resistors as heating elements, and a thermistor bead as a sensor. Objectives can be either dry, oil or glycerol-immersion and the short working distances needed with high numerical aperture lenses are not a problem because the cells are directly attached to the base of the chamber. The only practical difficulty is the tendency of the immersion fluid to run off the top of the lens, and sometimes a small plastic collar, or a ring of silicon grease, is needed to prevent this.

For experiments that are sensitive to mechanical vibration, for example where micro-pipettes are to be used, it is convenient to mount the microscope on an air-table, mechanically isolated from the excitation source with its cooling fans. This can be achieved by conducting light to the microscope through a fiber-optic bundle or a liquid light-guide (Figure 4), which has the added advantage that it diffuses the light from the arc, making it easier to distribute evenly over the field of view.

The last component of the optical system is a detector. The simplest form of detector is a photomultiplier tube, and for obtaining local mean activities, for example over a whole cell or a bundle of muscle fibres, it provides a fast, efficient method of signal collection. The technique is to place a pin-hole diaphragm in front of the tube and use the microscope to project an image of the cell onto the hole. Clearly alignment has to be carefully done, and one has to be confident that the cell will not move during the course of the experiment. Usually the photomultiplier will be connected as an analogue device, to an A/D converter and computer system; but for the best possible noise-immunity it can be connected instead to a pulse-height discriminator and

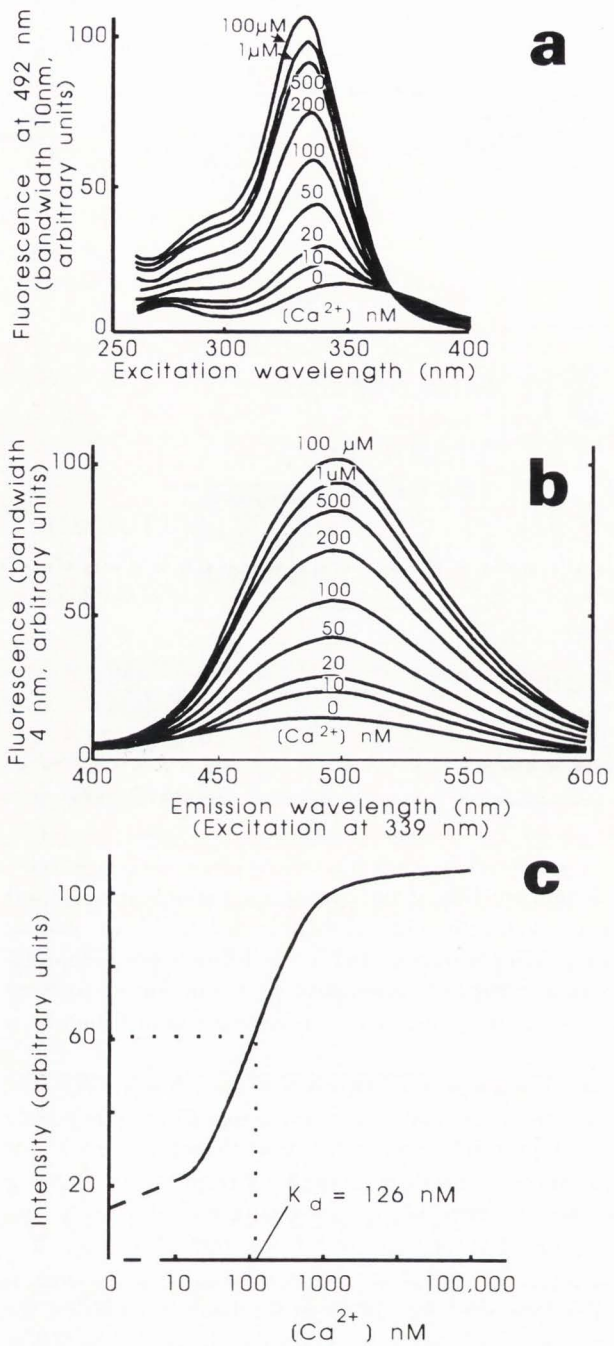

Figure 6: (a) Excitation and (b) Emission spectra of Quin-2 as a function of [Ca^{2+}] (20 μM Quin-2 , 120-135mM K^+, 20mM Na^+, 1mM free Mg^{2+}, pH 7.05, 37°C); (c) Emission at 492nm as a function of Ca^{2+}, with excitation at 335nm. (Data from Tsien et al., 1982).

counter which perform the same function as a band-pass optical filter by selecting only pulses generated by capture of photons of the appropriate wavelength. This technique of photon-counting is clearly analogous to the use of a pulse-height discriminator attached to an energy-dispersive X-ray spectrometer.

For detailed mapping, the photomultiplier is replaced by a camera, and for quantitative imaging work this needs to be an electronic camera capable of recording a linear representation of fluorescence intensity, which can be transmitted to an image-analysing computer. The best type of camera for this uses charge-coupled device, or CCD imaging (Tomkins and Lyons, 1993; Bookman and Horrigan, 1993), in which incident photons are focussed onto a silicon wafer carrying an array of electrostatic potential "wells" in which the resulting photo-electrons are trapped. At the end of each integration period the accumulated charges are gated out, line by line, and amplified to form a video signal. Because in most biological experiments the fluorescence intensities are very low - typically 10^{-5} lux or less - the camera needs to combine high sensitivity and low noise. For experiments where only a modest temporal resolution is needed, this is conveniently achieved by running the CCD at a low temperature, between -20 and -40° C (Lev-Ram *et al.*, 1992; Aikens, 1993; Law and O'Brien, 1993), using liquid nitrogen or a thermo-electric cooling device. This reduces spontaneous electron emissions to a very low level, 1 - 2 electrons per second in each collecting element, so that the camera can be allowed to collect photons for periods from 10 msec up to several seconds before gating out the image through an amplifier with suitable bandwidth. Alternatively, a micro-channel plate image intensifier can be coupled to the CCD. Incident photons are then converted to photoelectrons, which are amplified electronically 10^4 to 10^5 times before being converted back into photons by a phosphor optically coupled to the CCD. This arrangement is more expensive, and much noisier than a cooled CCD, but it provides a continuously updated image in a standard video signal, which is readily coupled to standard image acquisition hardware. Intensified CCD cameras are still preferred by a majority of users, particularly in applications where time resolution is important; but usage of cooled CCD cameras is increasing.

In either case, the camera is mounted on one of the standard camera or cine ports of the microscope, and its output is connected to an analogue-digital converter or "frame-grabber", interfaced to the computer to record each image as a string of numbers referred to as "pixels" (short for "picture elements"). Figure 5 is a summary diagram of a complete imaging system using two monochromators and a rotating mirror to switch between them. The whole system is controlled by the computer, and the creation or adaptation of software packages to provide sensible experimental protocols is not a trivial

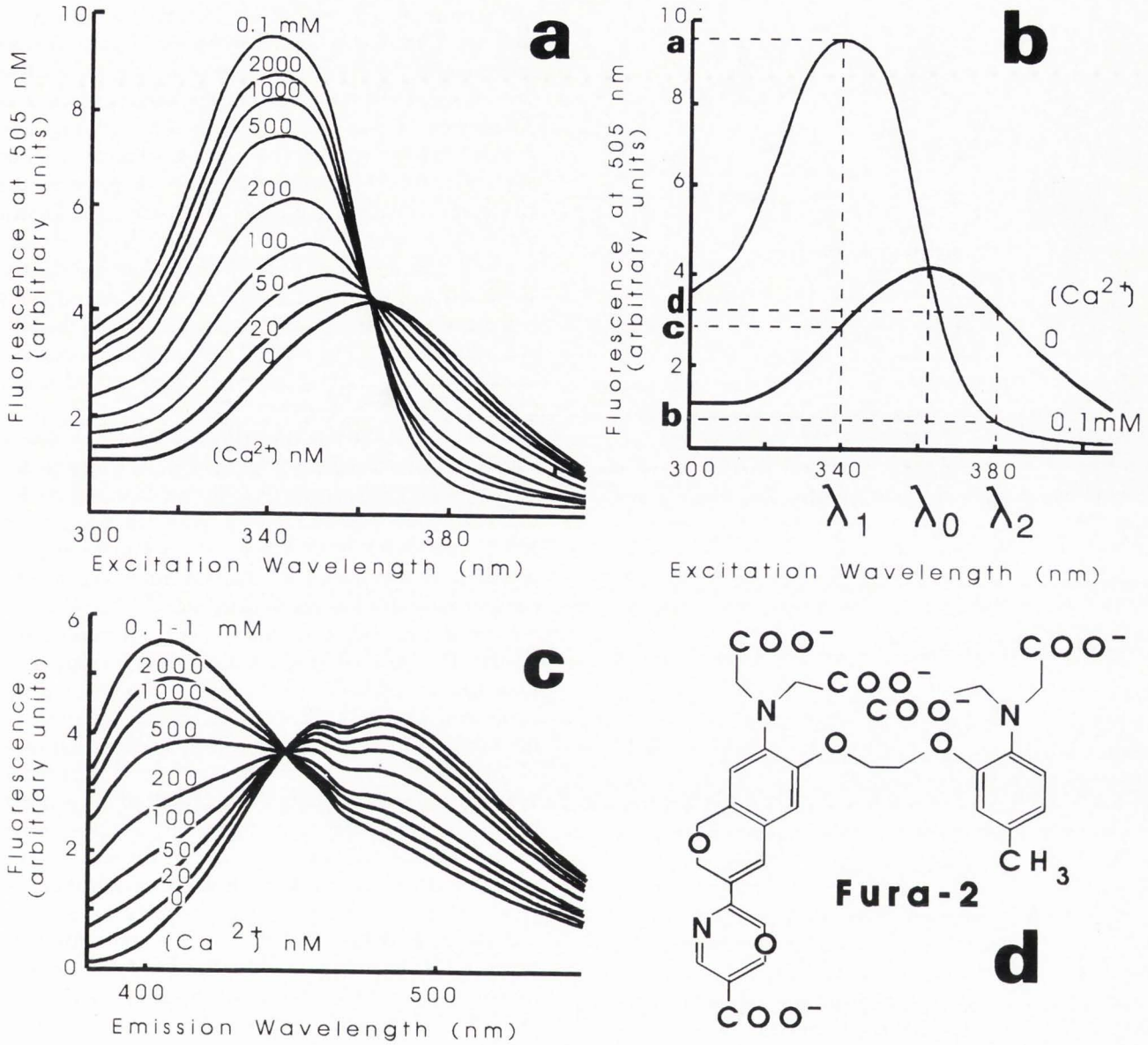

Figure 7: (a) Excitation spectrum of 1mM Fura-2 as a function of $[Ca^{2+}]$, in 115mM KCl, 20mM NaCl, 1mM free Mg^{2+}, pH 7.05, 37°C. (b) Excitation spectra of Fura-2 at zero and saturating $[Ca^{2+}]$. Ratio imaging data are derived as follows (see text): $R = I_{\lambda 1}/I_{\lambda 2}$, $R_{max} = a/b$, $R_{min} = c/d$, $S_{f2}/S_{b2} = d/b$. (c) Emission spectrum of 6 μM Indo-1 as a function of $[Ca^{2+}]$, under the same conditions as (a). (d) Molecular structure of Fura-2. (Spectral data from Grynkiewicz *et al.*, 1985)

task (Arndt-Jovin *et al.*, 1985; Mason *et al.*, 1993; Relf, 1993; Inoué, 1993).

As well as controlling the experiment, the function of the image analyser will be to convert the resulting fluorescent images into maps of the ionic activities under scrutiny. Before describing how this is done, it will be necessary to consider the properties of some of the fluorescent indicators now available, and the principles of quantitation.

Quantitation in Fluorescent Dye Imaging - the Ratio Method.

The basic requirement for an indicator dye is that its fluorescence intensity should vary, preferably as strongly as possible, with the activity of the ion being measured, and over the range of activities that is physiologically important. As an example, consider the calcium indicator known as Quin-2 (Tsien *et al.*, 1992). Figure 6 shows families of excitation and emission spectra for

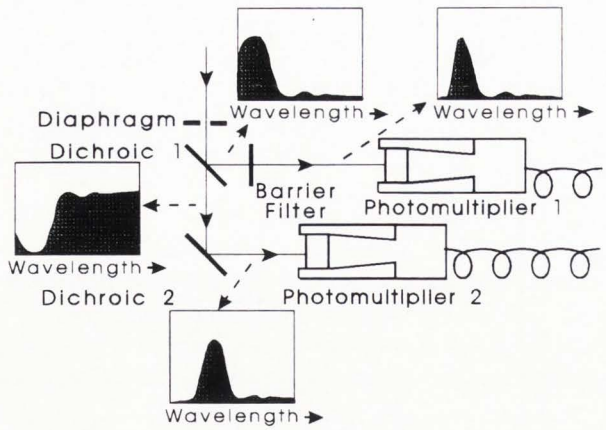

Figure 8: For fluorescence microscopy with dual-emission dyes, the fluorescence can be split into two wave-bands by two dichroic mirrors. The first mirror reflects wavelengths below a cut-off value into a long-pass filter which thus allows only a limited wavelength band to reach the first detector. Longer wavelengths are transmitted to the second mirror which has a higher cut-off and thus reflects a limited portion of the remaining light into the second detector.

Quin-2 at different calcium activities: the two extreme curves in each family correspond to those of the free and calcium-bound dye molecules, and a plot of peak emission intensity versus calcium activity shows that intermediate spectra come from mixtures of the two species, with a mid-point at the dissociation constant, K_d of the dye, and a useful range of calcium activities roughly centred on this value.

The problem in quantitative measurement is that, at given wavelengths of excitation and emission, the intensity of fluorescence detected from a dye at each point in the image will depend on several factors: the intensity of excitation light, the concentration of dye present, its extinction coefficient (i.e., the proportion of incident light that is absorbed), the quantum efficiency of fluorescence (the proportion of absorbed photons that give rise to fluorescence, as opposed to decay from the excited state by another route), overall sensitivity of the detecting device (which is taken as including the optical efficiency with which the image is projected onto it, and which may vary from point to point across the image) and the size of the excited micro-volume which contributes to that part of the image.

The intensity of excitation is generally controllable, though it may not be uniform across the field of view, and if the dye concentration is high some uncontrolled variations may occur due to absorption by the dye of a significant proportion of exciting radiation, so that not all dye molecules in a given path are exposed to the same intensity of excitation. Detector sensitivity is likewise controllable and can be calibrated. Optical properties of the dye can be measured from spectra like that shown. However the precise concentration and distribution of fluorescent dye within the cell are very difficult to control, particularly when chemical methods have been used to introduce it. The geometry of the excited micro-volume, although it depends in a known way upon the numerical aperture of the objective, is also not well determined because of uncertainties about the shape and optical properties of the dye-loaded cell. This is especially true in the frequent situation where the cells are small enough to be partly translucent to the exciting radiation, so that the actual excited volume depends critically on cell thickness.

One solution to this is to calibrate the dye *in situ* by waiting until the end of the experiment, then treating the cells to make them permeable to the ion in question - for example by permeabilizing them with detergent, or by adding ionophores such as ionomycin for calcium, or nigericin for hydrogen ions, then recording the fluorescence in a series of extracellular solutions of known ion activity and assuming equilibrium between outside and inside. This method is often used, and can produce reasonably reliable results, but errors can occur if the permeabilization procedure has not completely equalised the inside and outside ion activities, or (less controllably) if dye has become redistributed or lost from the cells during the experiment or as a result of the permeabilization; and of course it allows only a retrospective view of the actual ion activities during the experiment.

A much more powerful method of quantitation, known as the ratio method (Tsien *et al.*, 1985), is to use a dye which shows a significant spectral shift with increasing ionic activity, so that one part of the spectrum shows significant fluorescence changes with increasing ionic activity, while another part is unchanged or changes in the opposite direction. The ratio of fluorescence at two points in the spectrum can then give a measure of activity that is independent of dye concentration, optical path-length and excitation intensity (provided the latter is the same for both measurements). If calibration is done with an optical setup as nearly as possible the same as that used for the measurements, then any differences in excitation intensity and detector sensitivity will also cancel out.

An example of this is another calcium indicator, Fura-2 (Figure 7a; Grynkiewicz *et al.*, 1985; Tsien and Poenie, 1986). Here the excitation spectrum shows a shift in wavelength with calcium binding, with an isosbestic point at about 360 nm, while the wavelength of maximum emission (not shown) is almost constant. By exciting the dye alternately at 340 nm (the peak

wavelength for the calcium-bound form) and at 380 nm (where fluorescence decreases with calcium binding), and taking the ratio of fluorescence intensities measured at the same, optimal emission wavelength, an accurate measure of calcium activity is obtained. The method is analogous to the continuum method in X-ray microanalysis: the excited volume is directly equivalent in the two techniques, while beam current in X-ray microanalysis corresponds to the product of dye concentration and excitation intensity in fluorescence monitoring.

The formula used for ratio imaging, for a dye which binds to the indicated ion with 1:1 stoichiometry, is derived from the spectrum as follows (Figure 7b; Grynkiewicz *et al.*, 1985): the ratios for zero and saturating ion activities are measured, and taken as characteristic of the free and bound states of the dye; also required is the ratio of fluorescence intensities of the free and bound dye at the wavelength used to obtain the denominator of the ratio. At any given ionic activity, the proportions of free and bound dye molecules are determined by the standard chemical equilibrium equation for a dye (L) binding to an ion (X) with dissociation-constant K_d:

$$L + X \rightleftarrows LX \qquad (1)$$

$$K_d = [L].[X]/[LX] \qquad (2)$$

Combining this with the fluorescence calibration, we have:

$$[X] = K_d \frac{S_{f2} (R - R_{min})}{S_{b2} (R_{max} - R)} \qquad (3)$$

where R is the measured ratio, R_{max} and R_{min} are ratios for saturating and zero ion activity, and S_{f2}/S_{b2} is the ratio of free/bound intensity at the denominator wavelength λ_2.

To apply the formula, assuming the necessary calibration data are available, two images are recorded, and combined pixel by pixel. For "dual-excitation" dyes such as fura-2, where the calcium-dependent variation in fluorescence properties is mainly in the excitation spectrum, the two images must be acquired sequentially at different excitation wavelengths. Dual-excitation dyes are preferred for ratio imaging, because the excitation wavelength can easily be switched by a filter-wheel (Figure 1) or rotating mirror (Figure 2), allowing the same camera to acquire both images.

An alternative is to use a dye, such as Indo-1 (Figure 7c) (Grynkiewicz *et al.*, 1985), where the principal change due to ion binding is in the emission, rather than the excitation spectrum. This avoids the time-penalty of having to record two images sequentially, in order to produce one ratio image, because the emitted fluorescence can be split into two beams using dichroic mirrors, and the two wavelengths recorded simultaneously. However recording two images simultaneously at different emission wavelengths needs two cameras, which must be accurately aligned so that their images correspond, pixel-for-pixel. This is a formidable task, requiring the cameras to be aligned in all three dimensions, and although it has been done by mounting one camera on a micro-manipulator (Takamatsu and

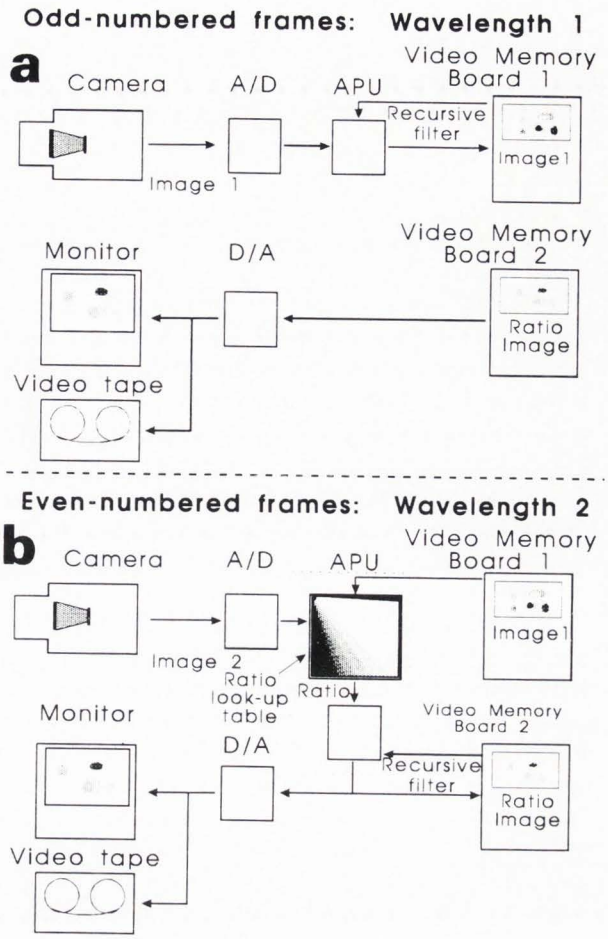

Figure 9: Real-time continuous ratio-imaging with IMAGINE. The chopper mirror or filter-wheel is synchronised to alternate between excitation wavelengths at each video frame. During odd-numbered frames, video memory board 1 collects data at one excitation wavelength, while board 2 simply refreshes the display. During even-numbered frames board 1 reads back the wavelength 1 image into the array-processor, which combines it with incoming data for wavelength 2 through the ratio look-up table., The resulting ratio image is stored on board 2, and output to the display and video tape.

Wier, 1990a,b) most imaging work using dual-emission dyes has been done at more limited spatial resolution using photomultipliers and a diaphragm to restrict the field over which fluorescence is averaged (Figure 8). It is relatively easy to align two photomultipliers with a dichroic beam-splitter to look at the same field simultaneously, and simply combine their outputs so that the ratio result is obtained immediately. This arrangement has the added advantage that its temporal resolution is no longer limited to video rate (33 or 40 msec per frame), so that events can be resolved as fast as the fluorescent dye will respond to changes in ion activity - for example the rate-constants for the Fura-2/calcium reaction are fast enough to give a temporal resolution of about 3 msec, depending on the conditions (Jackson *et al.*, 1987; Kao and Tsien, 1988; Garcia and Schneider, 1993).

Computation

Within the above constraints, the last decision to make in imaging work is, at what stage should the ratio calculation be done? An obvious, and easy solution is to acquire and store pairs of "raw" images, then apply the ratio formula at the end of the run to produce a new "animated" sequence describing the cells' behaviour (cf. Mason *et al.*, 1993; Relf, 1993). The alternative, if the hardware will do it, is to acquire one image (the denominator of the ratio), then input the second, numerator image, combining it with the first image at video-rate to give a "live" representation of ion activity, updated every two video frame-times (every 80 msec in Europe, 67 msec in the USA) as the experiment proceeds (O'Sullivan *et al.*, 1989; Moreton, 1992). The advantages of such a protocol are spectacular, in that the progress of an experiment can be watched all the time, and immediate decisions made. The live output image can be recorded continuously on video-tape, so that there is no danger of missing some critical event. The full potential of optical microscopy in observing the behaviour of living material is thereby realised. The disadvantages are firstly, that applying the ratio image formula to a whole image, which may contain a quarter of a million pixels, is a computationally expensive enterprise, and not many hardware systems have the capability to do it during the 30-40 msec time available per video frame. Secondly, applying the ratio formula to live data implies that the calibration values have all been determined in advance, so that there is no means of compensating for non-ideal behaviour of the particular dye sample in the particular intracellular environment, as can be done if calibration is performed after the experiment. Also, in situations where there is a need to compensate for uneven illumination by the exciting radiation, or where there is

(Figures 10 and 11 on facing page)

Figure 10: Calcium images of a single bovine adrenal chromaffin cell, loaded with fura-2 and excited alternately at 340 and 380 nm. Fluorescence at 510 nm was collected and combined to form a live ratio image of $[Ca^{2+}]$, using the IMAGINE system described in Figure 9. Individual frames were captured from the video recording at the times indicated, following application of 10 μM nicotine. $[Ca^{2+}]$ values are indicated by a pseudo-colour scale, as shown. The "wire-frame" plot at bottom right was formed by subtracting the basal image (top left), from the "1.5 sec" image. For details, see O'Sullivan *et al.* (1989).

Figure 11: (a) Calcium images of a single mouse oocyte, generated from fura-2 fluorescence as in Figure 10, and collected at 0, 1, 2, 3, 4 and 6 seconds from onset of the first calcium wave after fertilization of the egg by a sperm introduced into the medium. Fertilization induces a series of such waves, which in this instance begin at the lower end of the cell and spread throughout the cytosol. For details, see Cheek *et al.* (1993).

significant background fluorescence from optical components or culture-media, or autofluorescence from the cells themselves, it may be impractical to correct for these artifacts during a real-time computation. For best accuracy in quantitative imaging a non real-time method is probably best; but for observation of dynamic phenomena, a continuously updated image is more useful.

An interesting compromise was devised by Gustafson and Magnusson (1992), in which the two components of the ratio image are captured alternately and displayed simultaneously with a minimum of calculation, by connecting them to the red and green channels of a display monitor. Thus intensity ratios are displayed as different hues, while the net intensity (representing a combination of dye concentration and optical path-length) is displayed as overall brightness. This simple arrangement provides a continuously-updated visual impression of events, though off-line calculations still have to be used for full quantitation.

An important constraint upon the time resolution in fluorescence imaging arises from the statistical nature of the photon emission. Dye concentrations and illumination levels are limited by physiological considerations, so that a single video-rate fluorescent image usually contains insufficient photon-counts to provide a useful signal/noise ratio by itself, still less after being divided by another, equally noisy image. Some form of signal averaging is therefore needed, so that true video-rate, real-time imaging is not quite achievable. In non-real time applications the normal procedure is to collect and

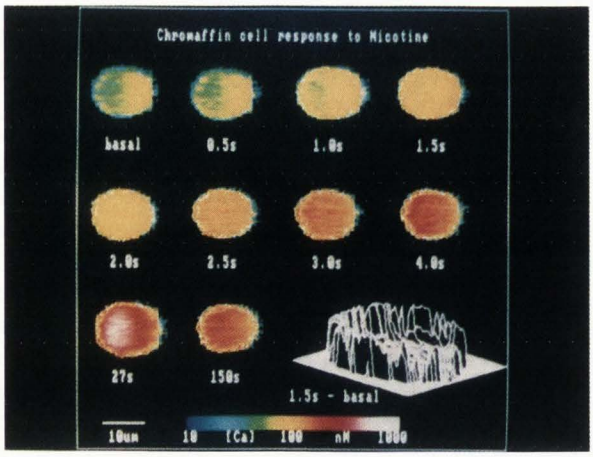

Fig. 10

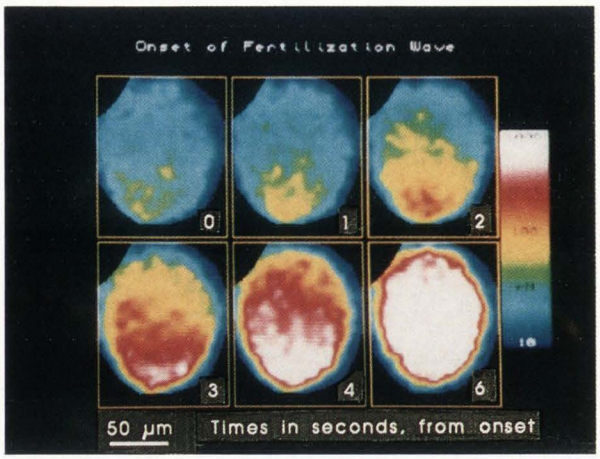

Fig. 11

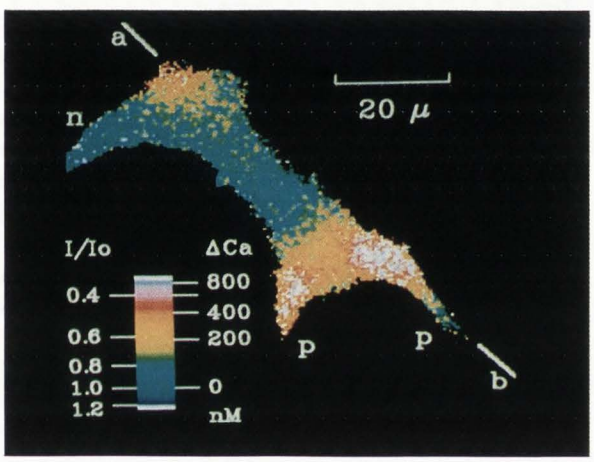

Fig. 12

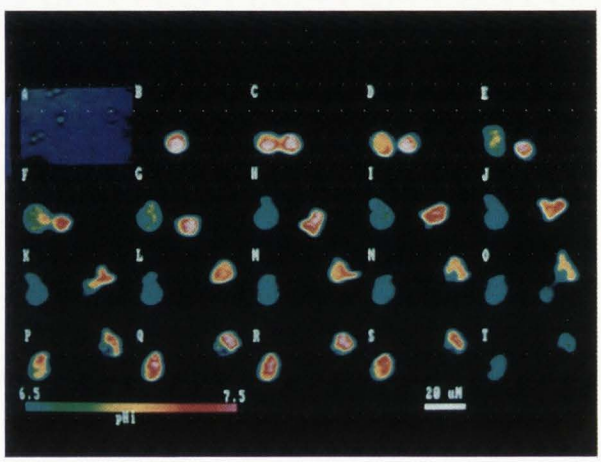

Fig. 13

Figure 12: Calcium hotspots at the neuronal growth cone revealed by fluorescence imaging. The figure shows the growth-cone of a single cultured N1E-115 neuroblastoma cell, loaded with fura-2 and excited at 380 nm. The image was produced by dividing the background-corrected video frame that began 0.5 s after the start of depolarization, by one acquired at the holding voltage, 0.5 s before depolarization. L-type calcium channels were activated by a 1 s voltage pulse from -40 mV to +10 mV. n - neurite leading to a cell body that is out of the field of view; p - process extending from the growth cone. (Reproduced with permission from Silver *et al. Nature* **343**, 751 - 754 (1990))

Figure 13: Illustration of intracellular pH changes in a pair of human polymorphonuclear neutrophil cells during landing and phagocytosis of yeast particles. The cells were loaded with pH indicator BCECF, and a ratio image was formed by exciting at 445 and 485 nm. Cells were initially in suspension, and are seen landing on a substrate containing yeast particles (A). Pictures were taken every 10 sec. The cell on the left lands first, and pH_i immediately drops as the cell begins to spread out from its original spherical shape. The cell on the right also begins to spread immediately, but at the same time starts to engulf a yeast particle (K), and during this process pH_i remains high, eventually dropping after phagocytosis is complete. Note that the fall in pH is not uniform, but begins in a small area round the phagosome (N,O). (P - S) calibration by addition of pH 7.5 buffer + ionophore, (T) calibration at pH 6.5.

Reproduced with permission from an experiment conducted at the University of Geneva by Jean-Marc Theler, Sergio Grinstein and Daniel Lew.

sum a set number of images (16, for example), change wavelengths, collect and sum another set, apply background-corrections if necessary, then form the ratio.

In real-time applications the best compromise is to maintain the denominator image as a running average or "recursively filtered" image. This is combined with each numerator image as it arrives, and the result in turn is recursively filtered with its predecessor (Moreton, 1992). The output then responds exponentially to step-changes in the input, providing the best compromise between responsiveness and noise-immunity. Systems for collecting and digitising video signals, or slow-scan outputs from cooled CCD cameras, converting them into two-dimensional numerical arrays of pixels, storing and processing the resulting images are many and varied, and time does not allow a detailed consideration here. Some, such as the Magical system from Joyce Loebl (Newcastle, UK), or the VIM system from Hamamatsu (Japan) have been specially programmed to allow controlled data acquisition, input of calibration data and construction of curves, from which ratio images can automatically be calculated. For real-time ratio imaging the choice of hardware is much more limited: one example is the system used in the Department of Zoology at Cambridge, based on the "Imagine" frame-store and image-processor, made in Cambridge by Synoptics Ltd. "Imagine" has a high-speed pixel processor that is fully programmable and can combine incoming video with stored images using a lookup table that has been pre-programmed to implement the ratio imaging formula, plus a few corrections for things like carry-over between images. Figure 9 summarises the operation of "Imagine" during the first and second member of each frame-pair. There are two independent video memory cards, which collect incoming data in turn, through the pixel array processor ("APU"). During the second frame, Board 1 also sends its stored data back to the APU, to be combined with incoming video to form the ratio image on Board 2. The result is a continuous video output representing ion activity, on a logarithmic scale and recursively filtered, usually with a time-constant of 200 msec (about 5 frame-times, or 2.5 frame-pairs). This we record on video tape, and can play back at leisure for later analysis.

Fluorescent Indicator Dyes

I have mentioned briefly the range of ions for which specific fluorescent indicators are now available. Table 1 summarises some of the dyes currently in use, showing the key points of their spectra, and their dissociation constants; for more detailed and tabulated information, see Minta and Tsien (1989); Verkman *et al.* (1989); Whitaker *et al.* (1991); Kasten (1993); Haughland (1993); Chen and Poenie (1993); Poenie and Chen (1993). As a rough guide, an indicator will provide useful information over activities ranging by about a factor of 10 on either side of the dissociation constant. In particular, note that there is a whole suite of indicators for calcium, developed by biochemists in response to the intense demand among biologists for information about intracellular calcium activity, which may range from a few tens of nanomolar in resting cells, up to 0.5 to 1 micromolar in cells responding, for example, to neurotransmitter or hormone signals, and locally higher still in contracting muscle cells. In extreme cases such as this it has been found necessary to use a mixture of indicators, for example Fura-2 and antipyrylazo III , to measure basal and peak stimulated levels respectively (Klein *et al.*, 1988; 1992; Simon *et al.*, 1991; Jacquemond and Schneider, 1992).

Figure 7d shows the structure of Fura-2 which, like that of most calcium indicators, is based on a tetra-carboxylic acid structure to give specific calcium binding, attached to a heterocyclic ring portion responsible for the fluorescence. Binding of calcium alters the electron distribution at the tetra-carboxylate end, and the effect feeds down to the fluorescent zone, altering the intensity or spectrum of fluorescence.

After calcium, the second most important imaging target is intracellular pH, for which a range of indicators is available, mainly based on the familiar fluorescein.

A topic that has not been mentioned, as it is only indirectly related to the optical methods, is the method of loading these indicators into the cells. In their nature as ion-binding molecules, most indicator dyes themselves exist in solution as ions, and are not therefore able to penetrate cell membranes. For large cells this is not a problem, because dye can readily be injected into the cytosol from a micropipette (e.g., Lev-Ram *et al.*, 1992; Nuccitelli *et al.*, 1993; Zoran *et al.*, 1993); or for cut muscle fibers it can be allowed to diffuse into the end (e.g., Gyorke and Palade, 1992). For cells being studied under whole-cell patch-clamp, where the cell membrane is sealed onto the end of a pipette and then ruptured inside the seal, so that the interior of the cell is continuous with that of the pipette, dye can simply be included in the pipette filling, and quickly equilibrates with the cytosol (e.g., Almers and Neher, 1985; Neher and Almers, 1986). Another method of insertion into small cells is to render them transiently permeable, for example by exposing them to a pulse of intense electric field in the presence of the dye (e.g., Iida *et al.*, 1990). After the pulse, cell membranes re-seal and their behaviour recovers. Plant cells may be sufficiently robust to be loaded at very low pH (4 - 4.5), where indicator dyes may be largely un-dissociated (Bush and Jones, 1987;

Table 1: Some fluorescent indicator probes for imaging intracellular ions.

Probe	Specific ion	Dissociation constant/P_k [1]	Wavelengths (nm) Excitation Low ion	Excitation High ion	Emission Low ion	Emission High ion	Quantitation method [2]
Calcium Crimson	Ca^{2+}	205 nM	588		611		x
Calcium Green-1		189 nM	506		534		x
Calcium Green-2		574 nM	506		531		x
Calcium Green-5N		3300 nM	506		531		x
Calcium Orange		328 nM	554		575		x
Fluo-3		316 nM	506		526		x
Fura-2		175 nM	380	340	510		Dual excitation
Fura Red		133 nM	472	436	640		Dual excitation
Indo-1		250 nM	346	330	408	495	Dual emission
Rhod-2		565 nM	553		576		x
Quin-2		126 nM	339		492		x
Mag-Fura-2	Mg^{2+}	1.5mM	370	330	511	491	Dual excitation
Mag-Fura-5		2.6 mM	369	332	505	482	Dual excitation
Mag-Indo-1		2.7 mM	349	330	476	417	Dual emission
Magnesium Green		0.9 mM	506		532		x
BCECF	H^+	pK 6.98	490	430	530		Dual excitation
Carboxy-SNAFL-2		7.74	476	530	620		Dual excitation
			552	530	620		
Carboxy-SNARF-2		7.61	522	530	592		Dual excitation
			582	530	592		
Carboxy-SNAFL-1		7.80	514		543	623	Dual emission
			540		622	582	
Carboxy-SNARF-1		7.62	540	574	587	630	Dual emission
SBFI	Na^+	7.4 mM	380	340	505		Dual excitation
PBFI	K^+	8.0 mM	346	334	551	525	x
SPQ	Cl^-	8.5 mM [3]	344		450		x
Other indicators for Calcium							
Aequorin	Ca^{2+}	(irreversible)	Luminescent		469		x
Arsenazo-III		40 μM [4]	574[5]	605	Dual absorbance		
		12 μM [4]	570[5]	650	Dual absorbance		
Antipyrylazo-III	Ca^{2+}	17,500μM [2 6]	550[5]	720	Dual absorbance		

[1] Values given here are intended mainly as a guide to the range of ion activities that can be usefully indicated by each dye. Dissociation constants are often strongly temperature-dependent, so that for accurate quantitative work a careful determination is needed under the particular experimental conditions used. Alternatively empirical calibration can be used, without specific knowledge of K_d.

[2] 'x' in this column indicates that no ratio method is available, and quantitation must rely on a simple measurement of fluorescence intensity, against a calibration scale.

[3] Deduced from the Stern-Volmer coefficient for quenching of fluorescence by Cl^-

[4] Depends on pH, and on $[Mg^{2+}]$ which can also be measured by suitable choice of wavelengths.

[5] The isosbestic wavelength (at which absorbance is independent of $[Ca^{2+}]$).

[6] Stoicheiometry of Ca^{2+} binding depends on concentration: value given is for a $Ca.(AP)_2$ complex.

Fricker *et al.*, 1993). For many dyes, however, a less invasive method is available, called ester loading (Tsien *et al.*, 1982; for a discussion of loading parameters, see Roe *et al.*, 1990; Williams *et al.*, 1993). In this method the dye is converted to its acetoxymethyl ester which, being non-ionic, is able to cross the cell membrane. Cells are exposed to a fine suspension of the ester which enters the cytosol, where it is cleaved by non-specific esterase enzymes which are present in most cells, and converted back to its ionised form which then becomes trapped and concentrated inside the cells. After 30 minutes or so, the concentration of dye inside the cells may be several times higher than that of the ester outside. The ester suspension is then washed away, and the cells are ready for imaging.

Applications

A brief look at some of the many applications of fluorescent ion monitoring in biology will serve to illustrate the wide-ranging use of the technique. Figure 10 shows a sequence of fluorescence images of a single bovine adrenal chromaffin cell, loaded with Fura-2 and excited alternately at 340 and 380 nm to form an image of calcium distribution by the ratio method, representing calcium activities in the range 10 to 1000 nM, as shown by the calibration "wedge" below. Images were captured from the recorded signal at the stated intervals after the cell had been exposed to nicotine (O'Sullivan *et al.*, 1989; Cheek *et al.*, 1989). Nicotine acts upon cholinergic receptors in the plasma membrane, causing depolarization and immediate influx of calcium. The "wire-frame" plot at bottom right was made by subtracting the "basal" image from the "1.5 second" image, and shows clearly how the initial calcium rise is restricted to the peripheral part of the cell. This peripherally-located calcium signal has been shown to be necessary in order to stimulate release of adrenalin from the cell, and it has been postulated that its efficacy is linked to the brief occurrence of very high calcium activity immediately beneath the plasma membrane; but unfortunately the spatial resolution if the technique is not adequate to detect this.

For other examples of spatial and temporal studies on calcium signalling, see Thomas *et al.* (1991); Wier and Blatter (1991).

Figure 11 shows a sequence of images of a mouse oocyte, also loaded with Fura-2, captured on the same imaging system as Figure 10 (Cheek *et al.*, 1993), and showing the wave of elevated calcium activity that sweeps across the cell after it has been fertilized by sperm introduced into the bathing medium. Again, the spatial resolution, which is particularly poor in these large, spheroidal cells, is insufficient to distinguish any details of the wave structure, and the picture may be compared with confocal images of oocytes which may show intricate circular or spiral patterns of wave propagation (Lechleiter *et al.*, 1991; Lechleiter and Clapham, 1992); at present, however, the epi-fluorescence method still has advantages of quantitative accuracy and temporal resolution which are not available in confocal imaging. Propagated calcium waves are seen in a number of diverse cell-types, and their mechanism and physiological function has been the subject of much research in recent years (see Berridge, 1993 for a recent review).

Figure 12, reprinted from Silver *et al.* (1990) by kind permission of the authors, probably illustrates the optimum spatial resolution available in epi-fluorescence imaging, using cultured neuroblastoma cells, again loaded with Fura-2, and imaged while under voltage-clamp. Here the thin-ness of the cells allows very localised calcium changes to be resolved, showing that L-type calcium channels in neural growth-cones appear to be clustered into a small number of "hot-spots", so that stimulation can cause large and tightly-localised calcium signals that are important for the control of neuronal development.

Figure 13 illustrates imaging of intracellular pH in neutrophils, using the fluorescein-based indicator BCE-CF, and is taken from some work with Dr Jean-Marc Theler and colleagues at the University of Geneva (Theler *et al.*, 1992). Here the stimulus is more physiological, involving interaction between the neutrophil and a yeast particle which is approached and ultimately engulfed by phagocytosis. The sequence clearly shows intracellular pH changes signalling these events.

For another example of imaging intracellular pH, this time in acid-secreting cells of the gastric mucosa, see Paradiso *et al.* (1987).

Scope and Limitations

This section will summarise the limitations of fluorescent ion monitoring, as compared with techniques based on the electron probe. Firstly, the scope of the technique is limited by the availability of fluorescent probes, to a small number of common inorganic ions, of which calcium is the most important. In this it is severely limited, by comparison with electron probe analysis; though biologists are now developing fluorescent antibodies that can be attached to a number of organic cell constituents, so that fluorescence imaging is beginning to provide dynamic information about the structure and molecular physiology of cells that is difficult to obtain by any other means.

A more serious limitation is the spatial resolution of

fluorescence imaging. The wavelength of the optical probe is of the order of 0.3 to 0.5 μm, which places an ultimate diffraction-limit on the resolution. A minute fluorescent particle can be localised with about this degree of precision; but in forming images of ion distribution the fluorescent indicator is normally diffusely distributed throughout the cell. Exciting radiation is also only poorly concentrated around the region of observation, so that dye above and below the plane of focus is also excited, and the image is seriously contaminated by out-of-focus fluorescence.

As shown in Figure 4 (a), the exciting radiation is focussed by the objective lens into a bi-conical region with a semi-verticle angle α, related to the numerical aperture of the lens by

$$\mu \sin \alpha = n \qquad (4)$$

where μ is refractive index of the medium, and n is the numerical aperture (cf. Moreton, 1992). Emitted radiation is collected from a similar bi-conical volume, so that the brightness of the image is proportional to the fourth power of the numerical aperture, and the effectiveness with which out-of-focus information is rejected is also much improved with high n.a. lenses. For example, for an objective with n.a. 1.3, operating in immersion-oil with refractive index 1.45, the semi-vertical angle of the cone will be 64° ; though of course this will change as the light is refracted through the coverslip and into the aqueous bathing medium. The process is directly analogous to beam-spread in electron-probe microanalysis. The net effect on spatial resolution depends on the precise geometry of the cells: thin cells give the best resolution, while very thick specimens such as oocytes give images with a resolution that is probably no better than 2 - 3 mm. One answer to this is to use a confocal microscope, with a pinhole diaphragm to reject out-of-focus information, and a laser-beam source which is scanned across the field in the manner of a scanning EM. However in epi-fluorescence imaging dramatic improvements can be obtained by collecting a stack of fluorescent images from planes above and below focus, and removing out-of-focus information by convoluting them with the point-spread function of the objective - that is, a corresponding stack of images derived from a single, point source (Fay *et al.*, 1989; Monck *et al.*, 1992). Both methods are effective and can improve the spatial resolution to 0.5 mm or better. Deconvolution requires much computation, however, and significantly increases the time taken to acquire a meaningful image, not least because each output image requires a stack of at least three input images, taken at different focal planes.

Because fluorescence imaging can be applied to living cells, temporal resolution is also important. As in electron-probe methods, the basic limit is set by the need to acquire sufficient photons per pixel to give reasonable counting statistics, plus a margin to allow for detector noise (though as counts from an X-ray spectrometer are being acquired from a fixed or frozen specimen, for strict comparison the relevant parameter in electron-probe microanalysis is the rate at which the tissue can be immobilised). The photon count available from a given dye depends on its concentration and efficiency of excitation, the excitation intensity and the overall sensitivity of the imaging detector.

If present at too high a concentration, the dye will buffer the ion under observation, so that physiological changes are damped or suppressed (e.g., Neher and Augustine, 1992). Increasing the excitation intensity can lead to bleaching of dye, with consequent loss of signal, or errors due to the formation of fluorescent products which are less sensitive to the ion of interest (e.g., Roe *et al.*, 1990). It can also lead to damage to the cell itself, either directly or from formation of toxic degradation products. This can be apparent through changes in cell behaviour, for example the cessation of spontaneous contraction in cardiac cells (Bals *et al.*, 1990), or of glucose-evoked calcium oscillations in pancreatic beta-cells (Grapengiesser, 1993). Bleaching and photodamage together are equivalent to beam damage in electron-probe microanalysis.

The imaging detector consists of the camera and microscope lens system. Good cameras achieve a quantum efficiency of about 10%. As detailed above, the proportion of emitted light reaching the camera depends strongly on the numerical aperture of the objective lens, but even with a lens of high numerical aperture light is collected from only a fraction of the available solid angle, and given other losses in the optics, overall efficiency is reduced to about 1%. In practical terms, with the best dyes available it is reasonable to expect a useful video image (512x512 pixels) in about 200 msec, at UV intensities which will allow continuous observation for up to 30 minutes. Using an optical magnification of 1000x, such an image will cover a field about 100 μm square.

For whole-cell measurements using a photomultiplier, of course, the number of photons available is much larger, and the time-resolution of the method becomes limited by the kinetics of the dye whose fluorescence can respond only as fast as it can bind or release the detected ions. For the calcium indicator fura-2, for example, the rate constants for calcium binding are such that a resolution of about 3 msec can be attained, fast enough to show calcium transients in

Table 2: Properties and limitations of optical fluoroscence and electron-probe X-ray microanalysis.

Technique	Optical fluorescence	Electron-probe X-ray microanalysis
Application	Specific ions & molecules, for which fluorescent probes are available.	All elements Z>2 (Li upwards)
Parameter measured	Thermodynamic activity	Volume concentration
Quantitation method	Dual wavelength ratiometric; or empirical calibration using buffers	Normalization against total sample mass
Tissue condition	Dynamic experiments on living cells under normal atmospheric conditions	Chemically or physically immobilized cells or tissues in vacuum
Tissue preparation	Cell monolayers, often in culture; whole tissues only if thin, or if examined by confocal microscopy	Fixed, freeze-dried or frozen sections; surface analysis of bulk tissue with limited resolution
Spatial resolution	2-4 μm in thick cells; improved in thinner specimens; <0.5 μm with confocal microscopy, or by deconvolution of epi-fluorescence images (at the expense of temporal resolution).	20-200 nm in sections, depending on thickness; >2 μm in bulk tissues, depending on electron and X-ray energy
Temporal resolution	1-10 msec for local averaging by photomultiplier (depends on dye kinetics); >200 msec in epi-fluorescence video imaging; ~1 sec on confocal microscopy	Signal acquisition may take many minutes, but tissues have been immobilised; rapid freezing may pin-point single events within fractions of a second
Detection limits	Activities of 10 nM may be detected, depending on the probe; for Ca^{2+} the minimum resolvable volume would then contain $3x10^{-21}$ g; given time, as few as 8 molecules of fluorescent dye can be detected.	$\sim 10^{-19}$ g, depending on element; but minimum detectable mass-fraction is ~0.01%, equivalent to 1mM concentration of Ca^{2+} or K^{+}

response to a single nerve action potential (Theler *et al.*, 1992).

As regards quantitative accuracy, fluorescence imaging suffers from the same limitations imposed by photon counting statistics and detector noise, as does electron-probe analysis. An additional source of error arises in determining the spectral properties of the fluorescent probe. As mentioned above, the ratiometric imaging method disposes of several unknowns, but in the end it is necessary to assume either that the spectral properties of the dye when in the cell are similar to those in free solution, where they can be measured in buffers containing known ion activities - equivalent to the standards in electron-probe microanalysis - or that the ion activity in the cells can be controlled by experimental manipulation, such as the use of ionophores, so that the dye can be calibrated *in situ* at the end of the experiment. Either of these assumptions is subject to considerable uncertainty, as the behaviour of fluorescent dyes is influenced by factors such as ionic strength, viscosity and polarity of the cellular medium, and in practice errors of 20 - 50% cannot be ruled out. For discussion of the possible sources of error, and of methods for correcting them, see Moore *et al.* (1990); Roe *et al.* (1990); Williams and Fay, (1990); Moreton, (1992); Bright (1993b); Hoyland (1993); Williams *et al.*

(1993). A particularly interesting method for minimising errors relies on the kinetics of the fluorescence process itself, by using a pulsed light-source and synchronised detection (Marriott *et al.*, 1991). Time-resolved fluorescence spectroscopy can also give useful information about the physico-chemical environment of the fluorophore: the subject is beyond the scope of the present paper, but for references see vandeVen and Gratton (1993); Keating and Wensel (1991); Oida *et al.* (1993).

Detection-limits in optical fluorescence imaging vary widely according to the species detected. Intracellular ions vary in activity from millimolar in the case of sodium, potassium, magnesium and chloride, to submicromolar in the case of calcium and hydrogen ions. However, because the fluorescent probes are introduced artificially into the cells, the quantity of probe available for detection is controllable, and is generally in the range of 10 - 100 μM. The range of measurable ion activities then depends purely on the dissociation constant of the dye-ion complex, which may be adjusted by the chemist to suit the biology. Different dyes are thus currently available to respond to calcium in ranges covering the physiological span from 10 nM to 1-2 μM, and for pH in the range 5-8. For calcium present at an activity of 100 nM, a micro-volume 2 μm cube will contain about $3x10^{-20}$ g of free ions.

Table 2 is a summary of properties, comparing optical fluorescence and electron-probe imaging methods. What is not apparent from the table, however, is the readiness with which optical imaging can be combined with other techniques such as electrophysiology (Niggli *et al.*, 1993), or direct intervention through release of calcium or other reagents locally into the cell by photolysis of "caged" precursors (Gurney, 1993; Kao and Adams, 1993). Such simultaneous monitoring and control of more than one parameter may offer a vital key to the understanding of many complex cellular signalling processes.

Acknowledgements

I am grateful to Dr T.R. Cheek, Dr O.M. McGuinness and Dr J-M Theler for permission to use the data shown in Figs. 10, 11 and 13 respectively, and to Dr S.R. Bolsover and the publishers of Nature for permission to reproduce Figure 12.

References

Adams SR, Harootunian AT, Buechler YJ, Taylor SS, Tsien RY (1991) Fluorescence ratio imaging of cyclic AMP in single cells. Nature **349**: 694 - 697.

Adams SR, Bacskai BJ, Taylor SS, Tsien RY (1993) Optical Probes for Cyclic AMP. In: *Fluorescent and Luminescent Probes for Biological Activity* (Mason WT, ed) Academic Press, London, Chapter 10, pp 133-149.

Aikens R (1993) Properties of Low-Light-Level Slow-Scan Detectors. In: *Fluorescent and Luminescent Probes for Biological Activity* (Mason WT, ed) Academic Press, London, Chapter 21, pp 277-286.

Almers W, Neher E (1985) The Ca signal from fura-2 loaded mast cells depends strongly on the method of dye loading. FEBS Lett **192**: 13-18.

Arndt-Jovin DJ, Robert-Nicoud M, Kaufman SJ, Jovin TM (1985) Fluorescence digital imaging microscopy in cell biology. Science **230**: 247-256.

Ashley CC, Ridgway EB (1970) On the relationships between membrane potential, calcium transient and tension in single barnacle muscle fibres. J Physiol **209**: 105-130.

Bals S, Bechem M, Paffhausen W, Pott L (1990) Spontaneous and experimentally evoked $[Ca^{2+}]_i$-transients in cardiac myocytes measured by means of a fast fura-2 technique. Cell Calcium **11**: 385-396.

Berridge MJ (1993) Inositol triphosphate and calcium signalling. Nature **361**: 315-325.

Bookman RJ, Horrigan FT (1993) Sampling Characteristics of CCD Video Cameras.
In: *Optical Microscopy: Emerging Methods and Applications* (Herman B, Lemasters JJ, eds) Academic Press, San Diego, Chapter 4, pp 115-131.

Bright GR (1993a) Multiparameter Imaging of Cellular Function. In: *Fluorescent and Luminescent Probes for Biological Activity* (Mason WT, ed) Academic Press, London, Chapter 14, pp 204-215.

Bright GR (1993b) Fluorescence Ratio Imaging: Issues and Artefacts. In: *Optical Microscopy: Emerging Methods and Applications* (Herman B, Lemasters JJ, eds) Academic Press, San Diego, Chapter 3, pp 87-114.

Brown JE, Brown PK, Pinto LH (1977) Detection of light-induced changes of intracellular ionized calcium concentration in Limulus ventral photoreceptors using arsenazo III. J Physiol **267**: 299-320.

Bush DS, Jones RL (1987) Measurement of cytoplasmic calcium in aleurone protoplasts using Indo-1 and Fura-2. Cell Calcium **8**: 455-472.

Campbell AK, Sala-Newby G (1993) Bioluminescent and Chemiluminescent Indicators for Molecular Signalling and Function in Living Cells. In: *Fluorescent and Luminescent Probes for Biological Activity* (Mason WT, ed) Academic Press, London, Chapter 5, pp 58-82.

Cheek TR, O'Sullivan AJ, Moreton RB, Berridge MJ, Burgoyne RD (1989) Spatial localization of the stimulus-induced rise in cytosolic free Ca^{2+} in bovine

adrenal chromaffin cells. FEBS Lett **247**: 429-434.

Cheek TR, McGuinness OM, Vincent C, Moreton RB, Berridge MJ, Johnson MH (1993) Fertilisation and thimerosal stimulate calcium spiking patterns in mouse oocytes but by separate mechanisms. Development **119**: 179-189.

Chen C-S, Poenie M (1993) New fluorescent probes for protein kinase C. Synthesis, characterization, and application. J Biol Chem **268**: 15812-15822.

Dipolo R, Requena J, Brinley Jr FJ, Mullins LJ, Scarpa A, Tiffert T (1976) Ionized calcium concentrations in squid axons. J gen Physiol **67**: 433-467.

Fay FS, Carrington W, Fogarty KE (1989) Three-dimensional molecular distribution in single cells analysed using the digital imaging microscope. J Microsc **153**: 133-149.

Florine-Casteel K, Lemasters JL, Herman B (1993) Video Imaging of Lipid Order. In: *Fluorescent and Luminescent Probes for Biological Activity* (Mason WT, ed) Academic Press, London, Chapter 32, pp 420-426.

Fricker M, Tester M, Gilroy S (1993) Fluorescence and Luminescence Techniques to Probe Ion Activities in Living Plant Cells. In: *Fluorescent and Luminescent Probes for Biological Activity* (Mason WT, ed) Academic Press, London, Chapter 28, pp 360-377.

Garcia J, Schneider MF (1993) Calcium transients and calcium release in rat fast-twitch skeletal muscle fibres. J Physiol **463**: 709-728.

Gorman ALF, Thomas MV (1978) Changes in the intracellular concentration of free calcium ions in a pacemaker neurone, measured with metallochromic indicator dye arsenazo III. J Physiol **275**: 357-376.

Grapengiesser E (1993) Cell photodamage, a potential hazard when measuring cytoplasmic Ca^{2+} with fura-2. Cell Struct Funct **18**: 13-17.

Grynkiewicz G, Poenie M, Tsien RY (1985) A new generation of Ca^{2+} indicators with greatly improved fluorescence properties. J Biol Chem **260**: 3440-3450.

Gurney AM (1993) Photolabile caged compounds. In: *Fluorescent and Luminescent Probes for Biological Activity* (Mason WT, ed) Academic Press, London, Chapter 26, pp 335-348.

Gustafson M, Magnusson K-E (1992) A novel principle for quantitation of fast intracellular calcium changes using fura-2 and a modified image processing system - applications in studies of neutrophil motility and phagocytosis. Cell Calcium **13**: 473-486.

Gyorke S, Palade P (1992) Calcium-induced calcium release in crayfish skeletal muscle. J Physiol **457**: 195-210.

Hahn KM, Waggoner AS, Taylor DL (1990) A calcium-sensitive fluorescent analog of calmodulin based on a novel calmodulin-binding fluorophore. J Biol Chem **265**: 20335-20345.

Haugland R (1993) Intracellular Ion Indicators. In: *Fluorescent and Luminescent Probes for Biological Activity* (Mason WT, ed) Academic Press, London, Chapter 3, pp 34-43.

Herman B, Lemasters JJ (eds) (1993) Optical Microscopy: Emerging Methods and Applications, Academic Press, Inc. San Diego.

Hoyland J (1993) Fluorescent Probes in Practice - Potential Artifacts. In: *Fluorescent and Luminescent Probes for Biological Activity* (Mason WT, ed) Academic Press, London, Chapter 16, pp 223-228.

Iida H, Yagawa Y, Anraku Y (1990) Essential role for induced Ca^{2+} influx followed by $[Ca^{2+}]_i$ rise in maintaining viability of yeast cells late in the mating pheromone response pathway. J Biol Chem **265**: 13391-13399.

Inoué T (1993) Image processing software for research microscopy: Requirement and design of the user interface. In: *Electronic Light Microscopy* (Shotton D, ed) Wiley-Liss, Inc., New York, Chapter 4, pp 95-103.

Jackson AP, Timmerman MP, Bagshaw CR, Ashley CC (1987) The kinetics of calcium binding to fura-2 and indo-1. FEBS Lett **216**: 35-39.

Jacquemond V, Schneider MF (1992) Effects of low myoplasmic Mg^{2+} on calcium binding by parvalbumin and calcium uptake by the sarcoplasmic reticulum in frog skeletal muscle. J gen Physiol **100**: 115-135.

Kao JPY, Tsien RY (1988) Ca^{2+} binding kinetics of fura-2 and azo-1 from temperature-jump relaxation measurements. Biophys J **53**: 635-639.

Kao JPY, Adams SR (1993) Photosensitive caged compounds: design, properties and biological applications. In: *Optical Microscopy: Emerging Methods and Applications* (Herman B, Lemasters JJ, eds) Academic Press, San Diego, Chapter 2, pp 27-114.

Kasten FH (1993) Introduction to Fluorescent Probes: Properties, History and Applications. In: *Fluorescent and Luminescent Probes for Biological Activity* (Mason WT, ed) Academic Press, London, Chapter 2, pp 12-33.

Keating SM, Wensel TG (1991) Nanosecond fluorescence spectroscopy. Emission kinetics of fura-2 in single cells. Biophys J **59**: 186-202.

Klein MG, Simon BJ, Szucs G, Schneider MF (1988) Simultaneous recording of calcium transients in skeletal muscle using high- and low-affinity calcium indicators. Biophys J **53**: 971-988.

Klein MG, Simon BJ, Schneider MF (1992) Effects of procaine and caffeine on calcium release from the sarcoplasmic reticulum in frog skeletal muscle. J Physiol **453**: 341-366.

Kok JW, Hoekstra D (1993) Fluorescent lipid analogues: Applications in Cell and Membrane Biology. In: *Fluorescent and Luminescent Probes for Biological Activity* (Mason WT, ed) Academic Press, London, Chapter 7, pp 100-119.

Kovacs L, Rios E, Schneider MF (1979) Calcium transients and intramembrane charge movement in skeletal muscle fibres. Nature **279**: 391-396.

Law GJ, O'Brien W (1993) A Small-Area Cooled CCD Camera and Software for Fluorescence Ratio Imaging. In: *Fluorescent and Luminescent Probes for Biological Activity* (Mason WT, ed) Academic Press, London, Chapter 13, pp 196-203.

Lechleiter J, Girard SE, Peralta EG, Clapham DE (1991) Spiral calcium wave propagation and annihilation in Xenopus laevis oocytes. Science **252**: 123-126.

Lechleiter JD, Clapham DE (1992) Molecular mechanisms of intracellular calcium excitability in X. laevis oocytes. Cell **69**: 283-294.

Lev-Ram V, Miyakawa H, Lasser-Ross N, Ross WN (1992) Calcium transients in cerebellar Purkinje neurons evoked by intracellular stimulation. J Neurophysiol **68**: 1167-1177.

Luby-Pheols K, Mujumdar S, Mujumdar RB, Emst LA, Galbraith W, Waggoner AS (1993) A novel fluorescence radiometric method confirms the low solvent viscosity of the cytoplasm. Biophys J **65**: 236-242.

Marriott G, Clegg RM, Arndt-Jovin DJ, Jovin TM (1991) Time resolved imaging microscopy. Biophys J **60**: 1374-1387.

Mason WT (1993) (ed) Fluorescent and Luminescent Probes for Biological Activity
Academic Press inc. London.

Mason WT, Hoyland J, Davison I, Carew M, Somasundaram B, Tregear R, Zorec R, Lledo PM, Shankar G, Horton M (1993) Quantitative Real-Time Imaging of Optical Probes in Living Cells. In: *Fluorescent and Luminescent Probes for Biological Activity* (Mason WT, ed) Academic Press, London, Chapter 12, pp 161-195.

Minta A, Tsien RY (1989) Fluorescent indicators for cytosolic sodium. J Biol Chem **264**: 19449-19457.

Monck JR, Oberhauser AF, Keating TJ, Fernandez JM (1992) Thin-section radiometric Ca^{2+} images obtained by optical sectioning of fura-2 loaded mast cells. J Cell Biol **116**: 745-759.

Moore EDW, Becker PL, Fogarty KE, Williams DA, Fay FS (1990) Ca^{2+} imaging in single living cells: theoretical and practical issues. Cell Calcium **11**: 157-179.

Moreton RB (1991) Optical Techniques and Ca^{2+} Imaging. In: *Cellular Neurobiology, a Practical Approach*, IRL Press, Oxford, Chapter 11, pp 205-222.

Moreton RB (1992) Single-cell imaging technology. In: *Neuromethods- Intracellular Messengers* (Boulton AA, Baker GB, Taylor CW, eds) vol 20, Humana Press inc., Totowa, New Jersey, 175-230.

Morris SJ (1993) Simultaneous Multiple Detection of Fluorescent Molecules: Rapid Kinetic Imaging of Calcium and pH in Living Cells. In: *Optical Microscopy: Emerging Methods and Applications* (Herman B, Lemasters JJ, eds) Academic Press, San Diego, Chapter 6, pp 177-212.

Neher E, Almers W (1986) Fast calcium transients in rat peritoneal mast cells are not sufficient to trigger exocytosis. EMBO J **5**: 51-53.

Neher E, Augustine GJ (1992) Calcium gradients and buffers in bovine chromaffin cells. J Physiol **459**: 273-301.

Niggli E, Hadley RW, Kirby MS, Lederer WJ (1993) Real-time Fluorescence Microscopy in Living Cells: Fluorescence Imaging, Photolysis of Caged Compounds, and Whole-Cell Patch Clamping. In: *Optical Microscopy: Emerging Methods and Applications* (Herman B, Lemasters JJ, eds) Academic Press, San Diego, Chapter 7, pp 213-235.

Nuccitelli R, Yim DL, Smart T (1993) The sperm-induced Ca^{2+} wave following fertilization of the *Xenopus* egg requires the production if $Ins(1,4,5)P_3$. Dev Biol **158**: 200-212.

O'Sullivan AJ, Cheek TR, Moreton RB, Berridge MJ, Burgoyne RD (1989) Localization and heterogeneity of agonist-induced changes in cytosolic calcium concentration in single bovine adrenal chromaffin cells from video imaging of fura-2. EMBO Journal **8**: 401-411.

Oida T, Sako Y, Kusumi A (1993) Fluorescence lifetime imaging microscopy (flimscopy). Methodology development and application to studies of endosome fusion in single cells. Biophys J **64**: 676-685.

Paradiso AM, Tsien RY, Machen TE (1987) Digital image processing of intracellular pH in gastric oxyntic and chief cells. Nature **325**: 447-450.

Ploem JS, Tanke HJ (1987) Introduction to fluorescence microscopy. Oxford University Press, London.

Ploem JS (1993) Fluorescence Microscopy. In: *Fluorescent and Luminescent Probes for Biological Activity* (Mason WT, ed) Academic Press, London, Chapter 1, pp 1-11.

Poenie M, Chen C-S (1993) New Fluorescent Probes for Cell Biology. In: *Optical Microscopy: Emerging Methods and Applications* (Herman B, Lemasters JJ, eds) Academic Press, San Diego, Chapter 1, pp 1-25.

Relf GT (1993) Digital Image Analysis: Software Approaches and Applications.
In: *Fluorescent and Luminescent Probes for Biological*

Activity (Mason WT, ed) Academic Press, London, Chapter 15, pp 216-221.

Roe MW, Lemasters JJ, Herman B (1990) Assessment of fura-2 for measurements of cytosolic free calcium. Cell Calcium **11**: 63-73.

Rost FWD (1991) Quantitative Fluorescence Microscopy. Cambridge University Press.

Sawin KE, Theriot JA, Mitchison TJ (1993) Photoactivation of Fluorescence as a Probe for Cytoskeletal Dynamics in Mitosis and Cell Motility. In: *Fluorescent and Luminescent Probes for Biological Activity* (Mason WT, ed) Academic Press, London, Chapter 31, pp 405-419.

Shimomura O, Johnson FH, Saiga Y (1962) Extraction, purification and properties of aequorin, a bioluminescent protein from the luminous hydromedusan, *Aequorea*. J Cell Comp Physiol **59**: 223-239.

Shotton D (ed) (1993) Electronic Light Microscopy, Wiley-Liss, inc. New York.

Silver RA, Lamb AG, Bolsover SR (1990) Calcium hotspots caused by L-channel clustering promote morphological changes in neuronal growth cones. Nature **343**: 751-754.

Simon BJ, Klein MG, Schneider MF (1991) Calcium dependence of inactivation of calcium release from the sarcoplasmic reticulum in skeletal muscle fibers. J gen Physiol **97**: 437-471.

Takamatsu T, Wier WG (1990a) High temporal resolution video imaging of intracellular calcium. Cell Calcium **11**: 111-120.

Takamatsu T, Wier WG (1990b) Calcium waves in mammalian heart: quantification of origin, magnitude, waveform, and velocity. FASEB Journal **4**: 1519-1525.

Taylor DL, Waggoner AS, Murphy RF, Lanni R, Birge RR (1986) Applications of Fluorescence in the Biomedical Sciences. Alan R Liss, New York.

Terasaki M (1993) Probes for the Endoplasmic Reticulum. In: *Fluorescent and Luminescent Probes for Biological Activity* (Mason WT, ed) Academic Press, London, Chapter 8, pp 120-124.

Theler J-M, Mollard P, Guerineau N, Vacher P, Pralong WF, Schlegel W, Wollheim CB (1992) Video imaging of cytosolic Ca^{2+} in pancreatic beta-cells stimulated by glucose, carbachol and ATP. J Biol Chem **267**: 18110-18117.

Thomas AP, Renard DC, Rooney TA (1991) Spatial and temporal organization of calcium signalling in hepatocytes. Cell Calcium **12**: 111-126.

Tomkins PR, Lyons A (1993) Properties of Low-Light-Level Video Frame Rate Cameras. In: *Fluorescent and Luminescent Probes for Biological Activity* (Mason WT, ed) Academic Press, London, Chapter 20, pp 264-276.

Tsien RY, Pozzan T, Rink TJ (1982) Calcium homeostasis in intact lymphocytes: cytoplasmic free calcium monitored with a new, intracellularly trapped fluorescent indicator. J Cell Biol **94**: 325-334.

Tsien RY, Rink TJ, Poenie M (1985) Measurement of cytosolic free Ca^{2+} in individual small cells using fluorescence microscopy with dual excitation wavelengths. Cell Calcium **6**: 145-157.

Tsien RY, Poenie M (1986) Fluorescence ratio imaging: a new window into intracellular ionic signaling. Trends Bioch Sci **11**: 450-455.

Tsien RY, Harootunian AT (1990) Practical design criteria for a dynamic ratio imaging system. Cell Calcium **11**: 93-109.

vandeVen M, Gratton E (1993) Time-resolved fluorescence life-time imaging. In: *Optical Microscopy: Emerging Methods and Applications* (Herman B, Lemasters JJ, eds) Academic Press, San Diego, Chapter 14, pp 373-402.

Verkman AS, Sellers MC, Chao AC, Lewy T, Ketchen R (1989) Synthesis and characterization of improved chloride sensitive fluorescent indicators for biological applications. Anal Biochem **178**: 355-361.

Whitaker JE, Haugland RP, Prendergast FG (1991) Spectral and photophysical studies of benzo(c)xanthene dyes: dual emission pH sensors. Anal Biochem **194**: 330-344.

Wier WG, Blatter LA (1991) Ca^{2+} - oscillations and Ca^{2+} - waves in mammalian cardiac and vascular smooth muscle cells. Cell Calcium **12**: 241-254.

Williams DA, Fay FS (1990) Intracellular calibration of the fluorescent calcium indicator fura-2. Cell Calcium **11**: 75-84.

Williams DA, Cody SH, Dubbin PN (1993) Introducing and calibrating fluorescent probes in cells and organelles. In: *Fluorescent and Luminescent Probes for Biological Activity* (Mason WT, ed) Academic Press, London, Chapter 25, pp 320-334.

Zoran MJ, Funte LR, Kater SB, Haydon PG (1993) Neuron-muscle contact changes presynaptic resting calcium set-point. Dev Biol **158**: 163-171.